Korean J. Chem. Eng., **20**(6), 1030-1036 (2003)

Characterization of Zirconium Sulfate Supported on TiO_2 and Activity for Acid Catalysis

Jong Rack Sohn† and Dong Gun Lee

Department of Industrial Chemistry, Engineering College, Kyungpook National University, Daegu 702-701, Korea
(*Received 8 August 2003 • accepted 24 September 2003*)

Abstract−A series of $Zr(SO_4)_2/TiO_2$ catalysts were prepared by impregnation of powder TiO_2 with an aqueous solution of zirconium sulfate. No diffraction line of zirconium sulfate was observed up to 30 wt%, indicating good dispersion of $Zr(SO_4)_2$ on the surface of TiO_2. The high catalytic activities of $Zr(SO_4)_2/TiO_2$ for both 2-propanol dehydration and cumene dealkylation were related to the increase of acidity and acid strength due to the addition of $Zr(SO_4)_2$. $Zr(SO_4)_2/TiO_2$ containing 25% zirconium sulfate and calcined at 400 °C exhibited maximum catalytic activities for 2-propanol dehydration and cumene dealkylation. The catalytic activities for these reactions were correlated with the acidity of catalysts measured by the ammonia chemisorption method.

Key words: $Zr(SO_4)_2/TiO_2$ Catalyst, Characterization, Acid Catalysis, 2-Propanol Dehydration, Cumene Dealkylation

INTRODUCTION

Solid acid catalysts play an important role in hydrocarbon conversion reactions in the chemical and petroleum industries, and in environmentally benign chemical processes [Cheung et al., 1995; Tanabe et al., 1989; Lee and Rhee, 1997; Sohn and Park, 2003]. Many kinds of solid acids have been found; their acidic properties on catalyst surfaces, their catalytic action, and the structure of acid sites have been elucidated for a long time, and those results have been reviewed [Arata, 1990; Sohn, 2003]. Among them, the strong acidity of zirconia-supported sulfate attracted much attention because of its ability to catalyze many reactions such as cracking, alkylation, and isomerization. The potential for a heterogeneous catalyst has yielded many papers on the catalytic activity of sulfated zirconia materials [Arata, 1990; Keogh et al., 1995; Figueras et al., 1997]. Sulfated zirconia incorporating Fe and Mn has been shown to be highly active for butane isomerization, catalyzing the reaction even at room temperature [Hsu et al., 1992; Adeeva et al., 1995]. Several investigators have reported that the addition of platinum to zirconia modified by sulfate ions enhances catalytic activity in the skeletal isomerization of alkanes without deactivation when the reaction is carried out in the presence of hydrogen [Ebitani et al., 1991; Vaudagna et al., 1997; Barton et al., 1999]. The high catalytic activity and small deactivation can be explained by both the elimination of the coke by hydrogenation and hydrogenolysis and the formation of Brönsted acid sites from H_2 on the catalysts [Ebitani et al., 1991]. Recently, others have reported zirconia-supported tungsten oxide as an alternative material in reaction requiring strong acid sites [Arata, 1990; Hino and Arata, 1987; Sohn and Park, 1998; Barton et al., 1999]. Several advantages of tungstate, over sulfate, as dopant include that it does not suffer from dopant loss during thermal treatment and it undergoes significantly less deactivation during catalytic reaction.

Many metal sulfates generate fairly large amounts of moderate or strong acid sites on their surfaces when they are calcined at 400-700 °C [Tanabe et al., 1989; Arata et al., 1990]. The acidic property of metal sulfate often gives high selectivity for diversified reactions such as hydration, polymerization, alkylation, cracking, and isomerization [Tanabe et al., 1989; Sohn and Park, 2000; Arata et al., 1990]. However, structural and physicochemical properties of supported metal sulfates are considered to be in different states compared with bulk metal sulfates because of their interaction with supports [Sohn and Park, 1998; Sohn et al., 2002]. Zirconium sulfate catalysts supported on TiO_2 have not been reported up to now.

This paper describes the characterization of zirconium sulfate supported on TiO_2 and activity for acid catalysis. The characterization of the samples was performed by means of Fourier transform infrared (FTIR), X-ray diffraction (XRD), Differential scanning calorimetry (DSC), and by the measurement of surface area. For the acid catalysis, the 2-propanol dehydration and cumene dealkylation were used as test reactions.

EXPERIMENTAL

The precipitate of $Ti(OH)_4$ was obtained by adding aqueous ammonia slowly into a mixed aqueous solution of titanium tetrachloride and hydrochloric acid at 60 °C with stirring until the pH of the mother liquor reached about 8 [Sohn and Bae, 2000]. The precipitate thus obtained was washed thoroughly with distilled water until chloride ion was not detected, and was dried at room temperature for 12 h. The dried precipitate was powdered below 100 mesh. Catalysts containing various zirconium sulfate contents were prepared by the impregnation of TiO_2 powder with an aqueous solution of $Zr(SO_4)_2 \cdot 4H_2O$ followed by calcining at different temperatures for 2 h in air. This series of catalysts is denoted by the weight percentage of zirconium sulfate. For example, 20-$Zr(SO_4)_2/TiO_2$ indicates the catalyst containing 20 wt% of $Zr(SO_4)_2$.

FTIR spectra were obtained in a heatable gas cell at room temperature by using a Mattson Model GL6030E spectrophotometer. The wafers contained about 9 mg/cm^2 self-supporting catalyst. Prior to obtaining of the spectra the samples were heated under vacuum

†To whom correspondence should be addressed.
E-mail: jrsohn@knu.ac.kr
‡This paper is dedicated to Professor Hyun Ku Rhee on the occasion of his retirement from Seoul National University.

at 25-400 °C for 1 h. Catalysts were checked in order to determine the structure of the prepared catalysts by means of a Philips X'pert-APD X-ray diffractometer, employing Ni-filtered Cu K_α radiation. DSC measurements were performed by a PL-STA model 1500H apparatus in air, and the heating rate was 5 °C/min. For each experiment 10-15 mg of sample was used.

The acid strength of catalyst was measured qualitatively by using a series of the Hammett indicators [Sohn et al., 1996; Sohn and Park, 1998]. The catalyst in a glass tube was pretreated at 500 °C for 1 h and filled with dry nitrogen. They were cooled to room temperature and filled with dry nitrogen. For the determination of acid strength of the catalyst, the color changes of indicators were observed by spot test. Chemisorption of ammonia was employed as a measure of acidity of catalysts. The amount of chemisorption was obtained as the irreversible adsorption of ammonia [Sohn and Ozaki, 1980; Sohn and Ryu, 1993; Sohn and Park, 2003]. Thus, the first adsorption of ammonia at 20 °C and 300 torr was followed by evacuation at 230 °C for 1 h and readsorption at 20 °C, the difference between two adsorptions at 20 °C giving the amount chemisorbed. The specific surface area was determined by applying the BET method to the adsorption of nitrogen at −196 °C.

2-propanol dehydration was carried at 160 and 180 °C in a pulse micro-reactor connected to a gas chromatograph. Fresh catalyst in the reactor made of 1/4 inch stainless steel was pretreated at 400 °C for 1 h in nitrogen atmosphere. Diethyleneglycol succinate on Simalite was used as packing material of the gas chromatograph and the column temperature was 180 °C for analyzing the product. Catalytic activity for 2-propanol dehydration was represented as mole of propylene converted from 2-propanol per gram of catalyst. Cumene dealkylation was carried out at 300-350 °C in the same reactor as above. Packing material for the gas chromatograph was Benton 34 on chromosorb W, and column temperature was 130 °C. Catalytic activity for cumene dealkylation was represented as mole of benzene converted from cumene per gram of catalyst. Conversion for both reactions was taken as the average of the first to sixth pulse values.

RESULTS AND DISCUSSION

1. Infrared Spectra of $Zr(SO_4)_2/TiO_2$

The infrared spectra of 25-$Zr(SO_4)_2/TiO_2$(KBr disc) calcined at different temperatures are given in Fig. 1. 25-$Zr(SO_4)_2/TiO_2$ calcined up to 600 °C showed infrared absorption bands at 1,232, 1,134, 1,047 and 1,003 cm^{-1} which are assigned to bidentate sulfate ion coordinated to the metal such as Zr^{4+} or Ti^{4+} [Sohn et al., 1995]. However, for the calcination of 700-800 °C, the infrared band by the sulfate ion disappeared because of the decomposition of sulfate ion, as shown in Fig. 1. These results are in good agreement with the data of DSC described below.

In general, for the metal oxides modified with the sulfate ion followed by evacuating above 400 °C, a strong bond assigned to S=O stretching frequency is observed in the range of 1,360-1,410 cm^{-1} [Saur et al., 1986; Yamaguchi, 1990; Sohn et al., 2002]. In this work, the corresponding band for samples exposed to air was not found because water molecules in air were adsorbed on the surfaces of the catalysts. These results are very similar to those reported by other authors [Sauer et al., 1986; Miao et al., 1996]. However, in a separate experiment infrared spectra of self-supported 10-$Zr(SO_4)_2/TiO_2$ after evacuation at 25-400 °C for 1 h were examined. As shown in Fig. 2, there were intense bands at 1,340-1,380 cm^{-1} accompanied

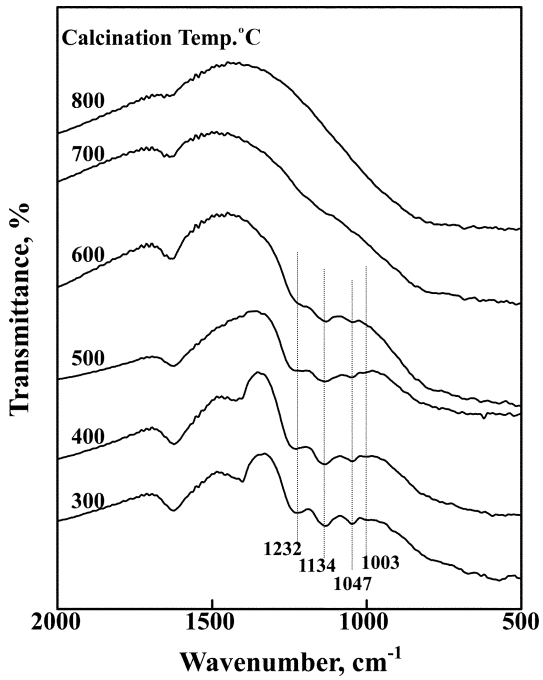

Fig. 1. Infrared spectra of 25-$Zr(SO_4)_2/TiO_2$ calcined at different temperatures for 2 h.

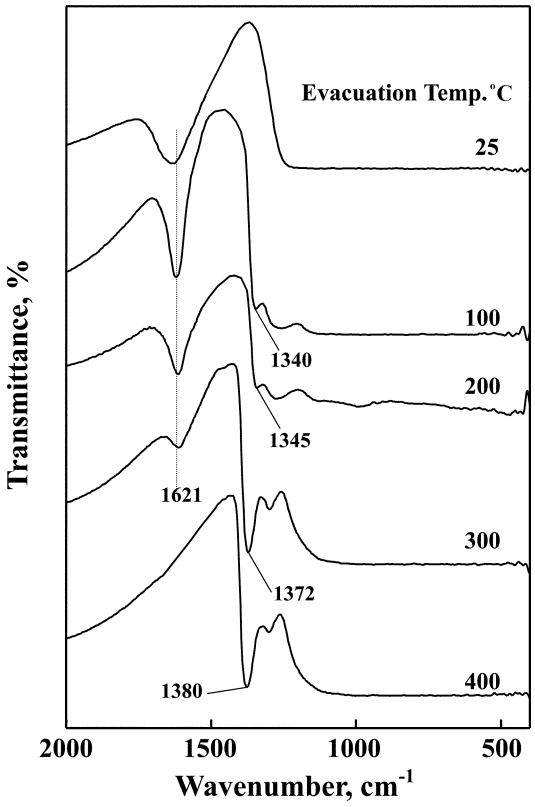

Fig. 2. Infrared spectra of 10-$Zr(SO_4)_2/TiO_2$ evacuated at different temperatures.

by broad and intense bands below 1,260 cm^{-1} due to the overlapping of the TiO_2 skeletal vibration, indicating the presence of different adsorbed species depending on the treatment conditions of the sulfated sample [Sohn et al., 2002; Sohn, 2003]. The bands at 1,340-1,380 cm^{-1} correspond to the asymmetric S=O stretching frequency of sulfate ion bonded to TiO_2 under the dehydrated condition, while the latter bands below 1,260 cm^{-1} are assigned to bidentate sulfate ion coordinated to TiO_2 [Jin et al., 1986; Yamaguchi, 1990]. These results are very similar to those of other workers [Jin et al., 1986; Saur et al., 1986].

However, the frequency shift of this band is different depending on the evacuation temperature, as shown in Fig. 2. The band at 1,621 cm^{-1} in Fig. 2 is assigned to the deformation vibration mode of the adsorbed water and the band intensity decreases with the evacuation temperature, showing complete disappearance at 400 °C. At 25 °C asymmetric stretching band of S=O bonds was not observed because the water molecules are adsorbed on the surface of 10-Zr $(SO_4)_2/TiO_2$ [Jin et al., 1986; Yamaguchi, 1990]. However, from 100 °C the band began to appear at 1,340 cm^{-1}. The band intensity increased with the evacuation temperature and the position of band shifted to a higher wave number. That is, the higher the evacuation temperature, the larger the shift of the asymmetric stretching frequency of the S=O bonds. It is likely that the surface sulfur complexes formed by the interaction of oxides with sulfate ions in highly active catalysts have a strong tendency to reduce their bond order by the adsorption of basic molecules such as H_2O [Jin et al., 1986; Yamaguchi, 1990; Sohn et al., 2003]. This frequency shift, corresponding to a decrease in the bond order of SO covalent bond and an increase in the partial charge on oxygen atom, is associated with the acid strength of the catalyst [Mia et al., 1996; Sohn and Park, 2003]. The electron structures of the sulfur complex before and after water adsorption may be illustrated as follows:

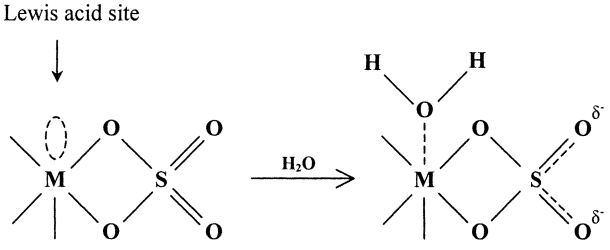

Consequently, as shown in Fig. 2, an asymmetric stretching band of S=O bonds for the sample evacuated at lower temperature appears at a lower frequency compared with that for the sample evacuated at higher temperature because of the adsorbed water. Therefore, it is obvious that the asymmetric stretching frequency of the S=O bonds is related to the acidic properties and catalytic activity discussed later.

2. Crystalline Structure of $Zr(SO_4)_2/TiO_2$

As shown in Fig. 3, for pure TiO_2 calcined in air at different temperatures for 2 h, X-ray diffraction data indicated an anatase phase at 400 °C, a two-phase mixture of the anatase and rutile forms at 500-700 °C, and a rutile phase at 800 °C. However, in the case of $Zr(SO_4)_2/TiO_2$, the crystalline structures of samples were different form those of the TiO_2 support.

The crystalline structure of 25-$Zr(SO_4)_2/TiO_2$ calcined at different temperatures for 2 h was also checked by X-ray diffraction. For

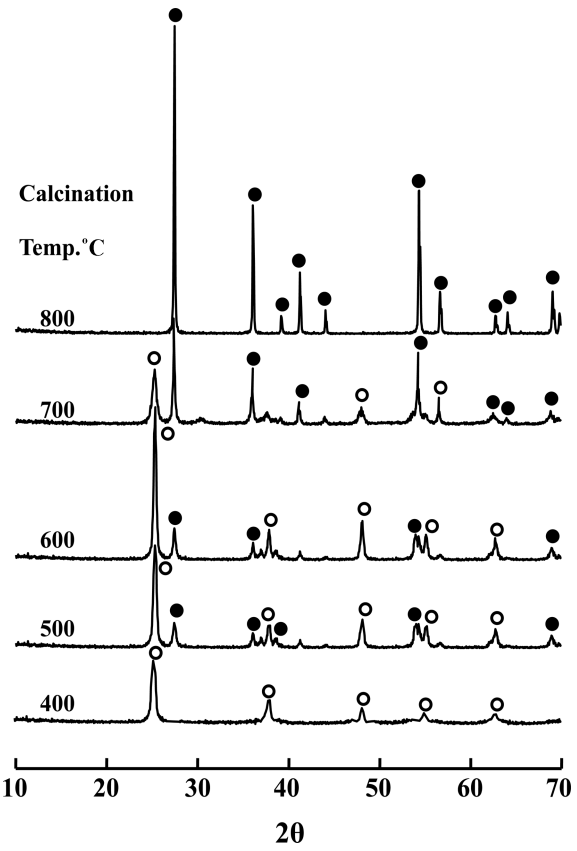

Fig. 3. X-ray diffraction patterns of TiO_2 calcined at different temperatures: ○, anatase phase of TiO_2; ●, rutile phase of TiO_2.

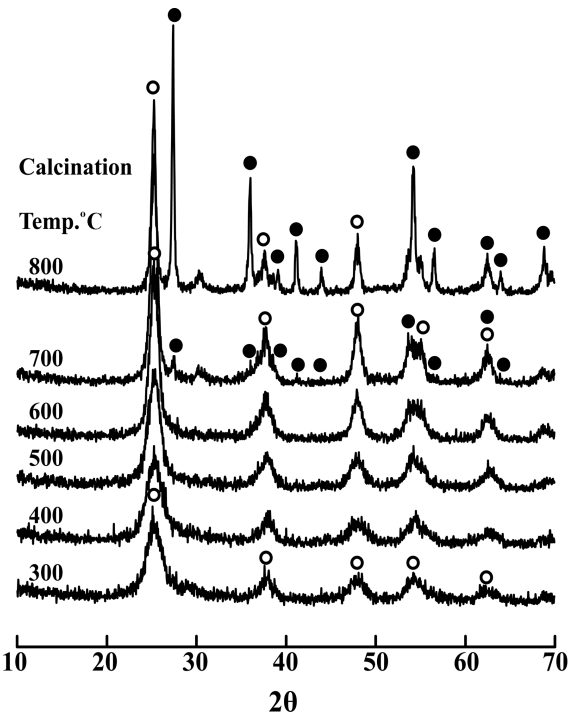

Fig. 4. X-ray diffraction patterns of 25-$Zr(SO_4)_2/TiO_2$ calcined at different temperatures: ○, anatase phase of TiO_2; ●, rutile phase of TiO_2.

the 25-$Zr(SO_4)_2/TiO_2$, as shown in Fig. 4, X-ray diffraction data indicated an anatase phase at 300-600 °C, showing an increased amount of anatase phase with the calcination temperature. However, at 700 °C a rutile phase of TiO_2 was observed due to the phase transition from anatase to rutile form.

Comparing Fig. 3 with Fig. 4, it is clear that the phase transition of TiO_2 in $Zr(SO_4)_2/TiO_2$ sample from anatase to rutile form is considerably delayed in comparison with the pure TiO_2 because of the interaction between $Zr(SO_4)_2$ and TiO_2 [Sohn et al., 2002]. In view of X-ray diffraction patterns, the calcination temperatures at which the rutile phase is observed initially are 500 °C for pure TiO_2 and 700 °C for 25-$Zr(SO_4)_2/TiO_2$, respectively. That is, the temperature for 25-$Zr(SO_4)_2/TiO_2$ is higher by 200 °C than that for pure TiO_2. For the same reason, only rutile phase in pure TiO_2 was observed at the calcination temperature of 800 °C, but a two-phase mixture of anatase and rutile forms in 25-$Zr(SO_4)_2/TiO_2$ sample was observed at the same temperature.

The XRD patterns of $Zr(SO_4)_2/TiO_2$ containing different zirconium sulfate contents and calcined at 400 °C for 2 h are shown in Fig. 5. No diffraction line of zirconium sulfate is observed at low $Zr(SO_4)_2$ loading up to 30 wt%, indicating good dispersion of Zr $(SO_4)_2$ on the surface of TiO_2 due to the interaction between them. For all $Zr(SO_4)_2/TiO_2$ samples, no rutile phase of TiO_2 was observed, indicating no phase transition of TiO_2 from anatase to rutile form at 400 °C. However, as shown in Fig. 5, the higher is the content of $Zr(SO_4)_2$, the lower is the amount of anatase phase for TiO_2, because the interaction between $Zr(SO_4)_2$ and TiO_2 prevents the formation of anatase TiO_2 [Sohn et al., 2002].

3. Thermal Analysis

To examine the thermal properties of precursors of $Zr(SO_4)_2/TiO_2$ samples more clearly, thermal analysis has been carried out and the results are illustrated in Fig. 6. For pure $Zr(SO_4)_2 \cdot 4H_2O$, the DSC curve shows four endothermic peaks below 400 °C due to water elimination, indicating that the dehydration of $Zr(SO_4)_2 \cdot 4H_2O$ occurs in four steps. The endothermic peak around 724 °C is due to the evolution of SO_3 decomposed from zirconium sulfate [Hua et al., 2000]. Decomposition of zirconium sulfate is known to begin at 700 °C, as shown in Fig. 6. For $Zr(SO_4)_2/TiO_2$ samples, the DSC patterns are somewhat different from that of $Zr(SO_4)_2 \cdot 4H_2O$. For all $Zr(SO_4)_2/TiO_2$ samples, the DSC curve showed broad endothermic peaks below 200 °C due to the elimination of adsorbed water without the dehydration in four steps as in the case of $Zr(SO_4)_2 \cdot 4H_2O$. The endothermic peak around 700 °C is due to the evolution of SO_3 decomposed from the sulfate ion bonded to the surface of TiO_2 [Hua et al., 2000].

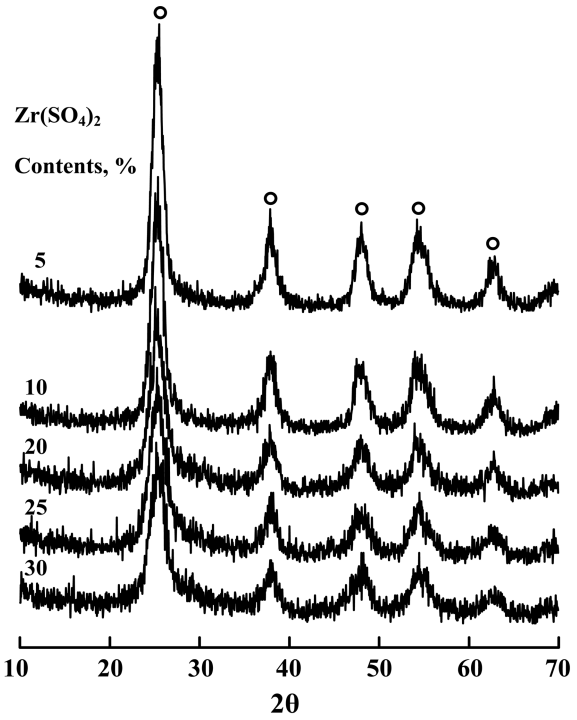

Fig. 5. X-ray diffraction patterns of $Zr(SO_4)_2/TiO_2$ having different $Zr(SO_4)_2$ contents and calcined at 400 °C: ○, anatase phase of TiO_2.

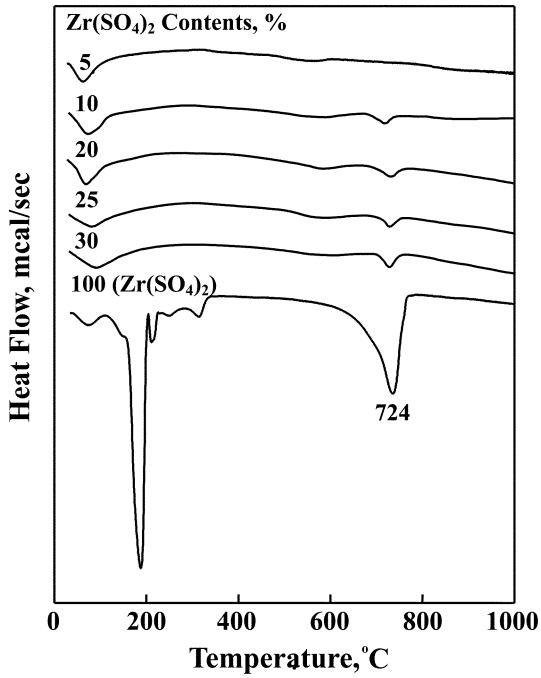

Fig. 6. DSC curves of $Zr(SO_4)_2/TiO_2$ precursors having different $Zr(SO_4)_2$ contents.

4. Surface Properties of Catalysts

It is necessary to examine the effect of zirconium sulfate on the surface properties of catalysts; that is, specific surface area, acid strength, and nature of acid centers (Brönsted or Lewis type). The specific surface areas of samples calcined at 400 °C for 2 h are listed in Table 1. Specific surface areas of $Zr(SO_4)_2/TiO_2$ samples are larger

Table 1. Surface area and acidity of $Zr(SO_4)_2/TiO_2$ catalysts calcined at 400 °C

Catalyst	Surface area (m^2/g)	Acidity (μmol/g)
TiO_2	125	188
5-$Zr(SO_4)_2/TiO_2$	150	307
10-$Zr(SO_4)_2/TiO_2$	214	336
20-$Zr(SO_4)_2/TiO_2$	187	340
25-$Zr(SO_4)_2/TiO_2$	158	353
30-$Zr(SO_4)_2/TiO_2$	130	302

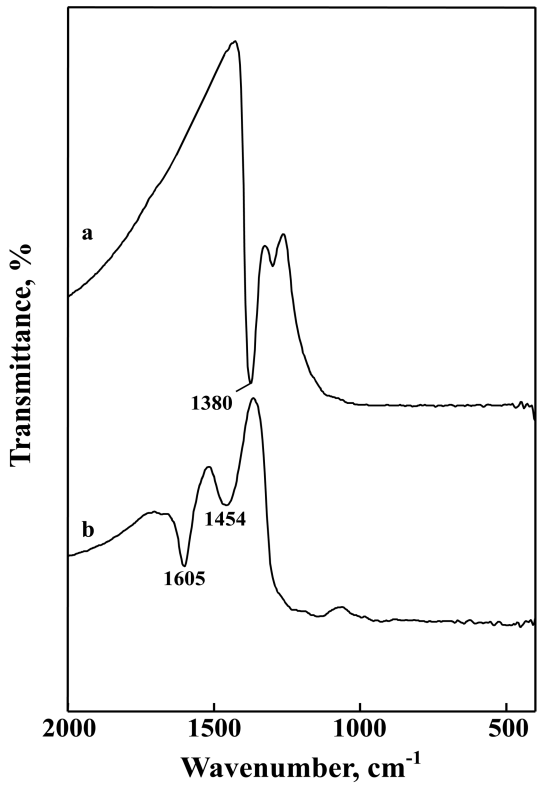

Fig. 7. Infrared spectra of NH_3 adsorbed on 10-$Zr(SO_4)_2/TiO_2$: (a) background of 10-$Zr(SO_4)_2/TiO_2$ after evacuation at 400 °C for 1 h, (b) NH_3 adsorbed on (a) after gas evacuation at 230 °C for 1 h.

than that of pure TiO_2 calcined at the same temperature, showing that surface area increases gradually with increasing zirconium sulfate content up to 10 wt%. It seems likely that the interaction between zirconium sulfate and TiO_2 protects catalysts from sintering [Sohn and Park, 1998].

Infrared spectroscopic studies of ammonia adsorbed on solid surfaces have made it possible to distinguish between Brönsted and Lewis acid sites [Sohn and Bae, 2000; Satsuma et al., 1988; Sohn and Park, 2003]. Fig. 7 shows the IR spectra of ammonia adsorbed on 10-$Zr(SO_4)_2/TiO_2$ samples evacuated at 400 °C for 1 h. The band at 1,454 cm^{-1} is the characteristic peak of an ammonium ion, which is formed on the Brönsted acid sites; the absorption peak at 1,605 cm^{-1} is contributed by ammonia coordinately bonded to Lewis acid sites [Sohn and Bae, 2000; Satsuma et al., 1988; Sohn and Park, 2003], indicating the presence of both Brönsted and Lewis acid sites on the surface of the 10-$Zr(SO_4)_2/TiO_2$ sample. Other samples having different zirconium sulfate content also showed the presence of both Lewis and Brönsted acids. As Fig. 7(a) shows, the intense band at 1,380 cm^{-1} after evacuation at 400 °C is assigned to the asymmetric stretching vibration of S=O bonds having a high double bond nature [Yamaguchi, 1990; Sohn et al., 1990; Sohn and Park, 2003]. However, the drastic shift of the IR band from 1,380 cm^{-1} to a lower wavenumber (not shown due to the overlaps of skeletal vibration bands of TiO_2) after ammonia adsorption [Fig. 7(b)] indicates a strong interaction between an adsorbed ammonia molecule and the surface complex. Namely, the surface sulfur compound in the highly acidic catalysts has a strong tendency to reduce the bond order of S=O from a highly covalent double-bond character to a lesser double-bond character when a basic ammonia molecule is adsorbed on the catalysts [Yamaguchi, 1990; Sohn and Park, 2003].

Acids stronger than $H_o \leq -11.93$, which corresponds to the acid strength of 100% H_2SO_4, are superacids [Tanabe et al., 1989; Yamaguchi, 1990; Olah et al. 1979; Arata, 1990]. The strong ability of the sulfur complex to accommodate electrons from a basic molecule such as ammonia is a driving force to generate superacidic properties [Tanabe et al., 1989; Yamaguchi, 1990; Sohn et al., 1990; Sohn and Park, 2003]. Consequently, $Zr(SO_4)_2/TiO_2$ catalysts would be solid superacids, in analogy with the case of metal oxides modified with a sulfate group [Sohn and Park, 2000; Sohn et al., 1995; Jin et al., 1986; Yamaguchi, 1990]. This superacidic property is attributable to the double bond nature of the S=O in the complex formed by the interaction between $Zr(SO_4)_2$ and TiO_2 [Tanabe et al., 1989; Jin et al., 1986; Yamaguchi, 1990]. $Zr(SO_4)_2/TiO_2$ samples after evacuation at 400 °C for 1 h was also examined by color change method, using Hammet indicator in sulfuryl chloride [Sohn et al., 1996; Sohn and Ryu, 1993]. The samples were estimated to have $H_o \leq -14.5$ indicating the formation of superacidic sites. In other words, the acid strength of $Zr(SO_4)_2/TiO_2$ becomes stronger by the inductive effect of S=O in the complex.

5. Catalytic Activities for Acid Catalysis

The catalytic activities for the 2-propanol dehydration were measured, and the results are illustrated as a function of $Zr(SO_4)_2$ content in Fig. 8, where reaction temperatures are 160-180 °C. In view of Table 1 and Fig. 8, the variations in catalytic activity for 2-propanol dehydration are well correlated with the changes of their acidity, showing the highest activity and acidity for 25-$Zr(SO_4)_2/TiO_2$. It has been known that 2-propanol dehydration takes place very readily on weak acid sites [Sohn et al., 2002; Decanio et al., 1986]. Good correlations have been found in many cases between the acidity

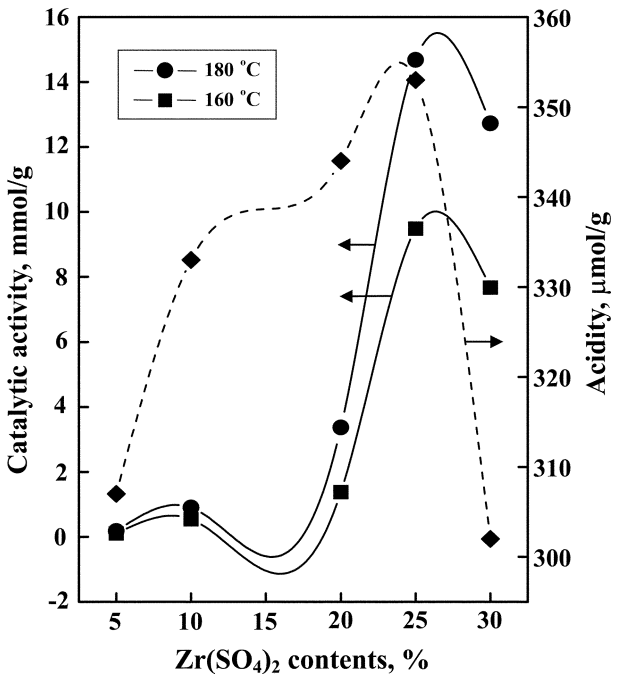

Fig. 8. Catalytic activities and acidity of $Zr(SO_4)_2/TiO_2$ for 2-propanol dehydration as a function of $Zr(SO_4)_2$ content.

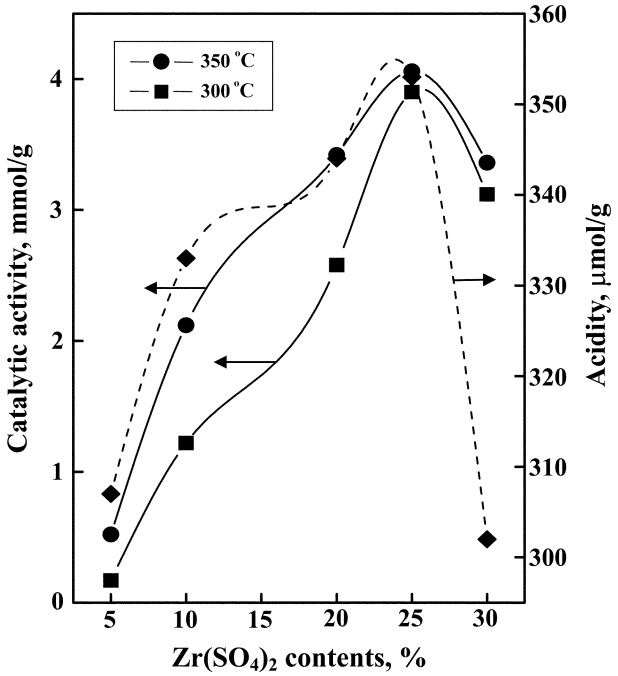

Fig. 9. Catalytic activities and acidity of $Zr(SO_4)_2/TiO_2$ for cumene dealkylation as a function of $Zr(SO_4)_2$ content.

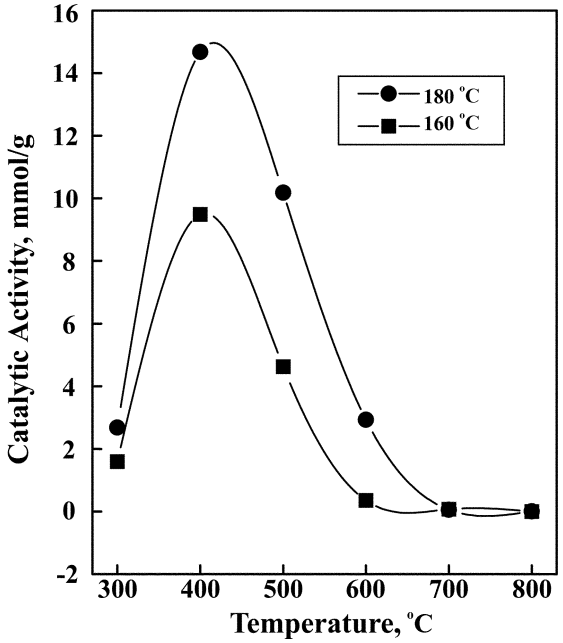

Fig. 10. Catalytic activities of 25-$Zr(SO_4)_2/TiO_2$ for 2-propanol dehydration as a function of calcination temperature.

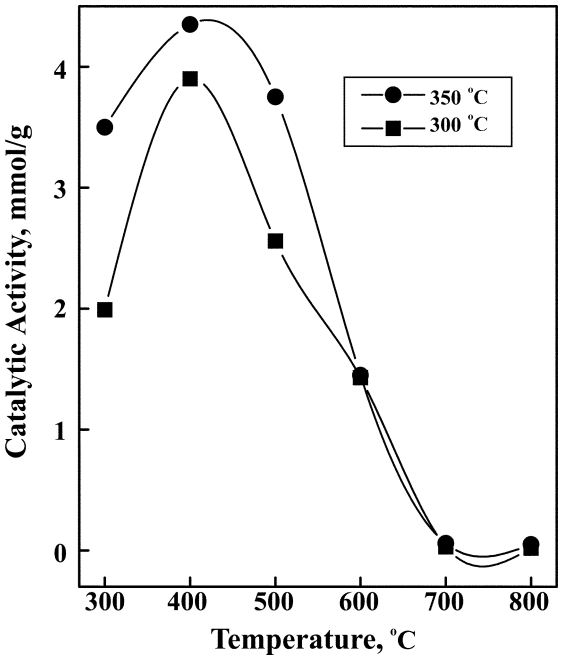

Fig. 11. Catalytic activities of 25-$Zr(SO_4)_2/TiO_2$ for cumene dealkylation as a function of calcination temperature.

and the catalytic activities of solid acids. For example, the rates of both the catalytic decomposition of cumene and the polymerization of propylene over SiO_2-Al_2O_3 catalysts were found to increase with increasing acid amounts at strength $H_o \leq +3.3$ [Tanabe, 1970]. It was also reported that the catalytic activity of nickel silicates in the ethylene dimerization as well as in the butene isomerization was closely correlated with the acidity of the catalyst [Sohn and Ozaki, 1980; Sohn et al., 2002].

Cumene dealkylation takes place on relatively strong acid sites of the catalysts [Sohn et al., 2002; Decanio et al., 1986]. Catalytic activities for cumene dealkylation against $Zr(SO_4)_2$ content are presented in Fig. 9, where reaction temperature is 300-350 °C. Comparing Table 1 and Fig. 9, the catalytic activities are also correlated with the acidity. The correlation between catalytic activity and acidity holds for both reactions, cumene dealkylation and 2-propanol dehydration, although the acid strength required to catalyze acid reactions is different depending on the type of reactions. Therefore, the highest catalytic activities of catalyst containing 25% $Zr(SO_4)_2$ for these reactions can be explained in terms of the highest acidity of this catalyst. As seen in Figs. 8 and 9, the catalytic activity for cumene dealkylation, in spite of higher reaction temperature, is lower than that for 2-propanol dehydration.

Catalytic activities of 25-$Zr(SO_4)_2/TiO_2$ are plotted as a function of calcination temperature for 2-propanol dehydration in Fig. 10. The activities increased with the calcination temperature, giving a maximum at 400 °C and then the activities decreased. Catalytic activities of 25-$Zr(SO_4)_2/TiO_2$ for cumene dealkylation are also plotted as a function of calcination temperature in Fig. 11. The activities also exhibited a maximum at 400 °C. The decrease of activity for both reactions above 400 °C can be probably attributed to the fact that the surface area and acidity above 400 °C decrease with the calcination temperature.

CONCLUSIONS

This paper has shown that a combination of FTIR, DSC, and XRD can be used to perform the characterization of $Zr(SO_4)_2/TiO_2$ prepared by the impregnation of powdered TiO_2 with zirconium sulfate aqueous solution followed by calcining in air. No diffraction line of $Zr(SO_4)_2$ was observed up to 30 wt%, indicating good dispersion of $Zr(SO_4)_2$ on the surface of TiO_2. The higher is the content of $Zr(SO_4)_2$, the lower is the amount of anatase TiO_2 phase for

$Zr(SO_4)_2/TiO_2$ because of the interaction between $Zr(SO_4)_2$ and TiO_2. 25-$Zr(SO_4)_2/TiO_2$ calcined at 400 °C exhibited the highest catalytic activity for both reactions, cumene dealkylation and 2-propanol dehydration. The shifts of S=O stretching frequency for sulfate group are related to the acidic properties and catalytic activities for acid catalysis. The high catalytic activity of $Zr(SO_4)_2/TiO_2$ was related to the increase of acidity and acid strength owing to the addition of $Zr(SO_4)_2$. The correlation between catalytic activity and acidity holds for both reactions although the acid strength required to catalyze acid reactions is different depending on the type of reactions.

ACKNOWLEDGMENTS

This work was supported by grant No. (R05-2003-000-10074-0) from the Basic Research Program of the Korea Science Engineering Foundation. We wish to thank Korea Basic Science Institute (Daegu Branch) for the use of X-ray diffractometer.

REFERENCES

Adeeva, V., de Haan, J. W., Janchen, J., Lei, G, D., Schunemann, V., van de Ven, L. J. M., Sachtler, W. M. N. and van Santen, R. A., "Acid Sites in Sulfated and Metal-promoted Zirconium Dioxide Catalysts," *J. Catal*., **151**, 364 (1995).

Arata, K., "Solid Superacids," *Adv. Catal*., **37**, 165 (1990).

Arata, K., Hino, H. and Yamagata, N., "Acidity and Catalytic Activity of Zirconium and Titanium Sulfates Heat-Treated at High Temperature. Solid Superacid Catalysts," *Bull Chem. Soc. Jpn*., **63**, 244 (1990).

Barton, D. G., Soled, S. R., Meitzner, G. D., Fuentes, G. A. and Iglesia, E., "Structural and Catalytic Characterization of Solid Acids Based on Zirconia Modified by Tungsten Oxide," *J. Catal*., **181**, 57 (1999).

Cheung, T. K., d'Itri, J. L., Lange, F. C. and Gates, B. C., "Neopentane Cracking Catalyzed by Iron and Manganese-promoted Sulfated Zirconia," *Catal. Lett*., **31**, 153 (1995).

DeCanio, S. J., Sohn, J. R., Fritz, P. O. and Lunsford, J. H., "Acid Catalysis by Dealuminated Zeolite-Y," *J. Catal*., **101**, 132 (1986).

Ebitani, K., Konish, J. and Hattori, H., "Skeletal Isomerization of Hydrocarbons over Zirconium Oxide Promoted by Platinum and Sulfate Ion," *J. Catal*., **130**, 257 (1991).

Figueras, F., Coq, B., Walter, C. and Carriat, J. Y., "Hydroconversion of Methylcyclohexane on Bifunctional Sulfated Zirconia-supported Platinum Catalysts," *J. Catal*., **169**, 103 (1997).

Hino, M. and Arata, K., "Synthesis of Solid Superacid of Tungsten Oxide Supported on Zirconia and its Catalytic Action for Reactions of Butane and Pentane," *J. Chem. Soc., Chem. Commun*., 1259 (1988).

Hsu, C. Y., Heimbuch, C. R., Armes, C. T. and Gates, B. C., "A Highly Active Solid Superacid Catalyst for n-Butane Isomerization: a Sulfated Oxide Containing Iron, Manganese and Zirconium," *J. Chem. Soc., Chem. Commun*., 1645 (1992).

Hua, W., Xia, Y., Yue, Y. and Gao, Z., "Promoting Effect of Al on SO_4^{2-}/M_xO_y (M=Zr, Ti, Fe) Catalysts," *J. Catal*., **196**, 104 (2000).

Jin, T., Yamaguchi, T. and Tanabe, K., "Mechanism of Acidity Generation on Sulfur-Promoted Metal Oxides," *J. Phys. Chem*., **90**, 4794 (1986).

Keogh, R. A., Srinivasan, R. and Davis, B. H., "Pt-SO_4^{2-}-ZrO_2 Catalysts the Impact of Water on Their Activity for Hydrocarbon Conversion," *J. Catal*., **151**, 292 (1995).

Lee, J. K. and Rhee, H. K., "Effect of Metal/Acid Balance in Pt-loaded Large Pore Zeolites on the Hydroisomerization of n-Hexane and n-Heptane," *Korean J. Chem. Eng*., **14**, 451 (1997).

Miao, C., Hua, W., Chen, J. and Gao, Z., "Studies on SO_4^{2-} Promoted Mixed Oxide Superacids," *Catal. Lett*., **37**, 187 (1996).

Olah, G. A., Prakash, G. K. S. and Sommer, J., "Superacids," *Science*, **206**, 13 (1979).

Satsuma, A., Hattori, A., Mizutani, K., Furuta, A., Miyamoto, A., Hattori, T. and Murakami, Y., "Surface Active Sites of V_2O_5-WO_3 Catalysts," *J. Phys. Chem*., **92**, 6052 (1988).

Saur, O., Bensitel, M., Saad, A. B. M., Lavalley, J. C., Tripp, C. P. and Morrow, B. A., "The Structure and Stability of Sulfated Alumina and Titania," *J. Catal*., **99**, 104 (1986).

Siriwardane, R. V., Poston, Jr., J. A., Fisher, E. P., Shen, M.-S. and Miltz, A. L., "Decomposition of the Sulfates of Copper, Iron (II), Iron (III), Nickel, and Zinc: XPS, SEM, DRIFTS, XRD, and TGA Study," *Appl. Surf. Sci*., **152**, 219 (1999).

Sohn, J. R., "Progress in Solid Superacid Catalyst," *J. Ind. Eng. Chem*., **10**, 1 (2004).

Sohn, J. R. and Bae, J. H., "Characterization of Tungsten Oxide Supported on TiO_2 and Activity for Acid Catalysis," *Korean J. Chem. Eng*., **17**, 86 (2000).

Sohn, J. R., Cho, S. G., Pae, Y. I. and Hayashi, S., "Characterization of Vanadium Oxide-zirconia Catalyst," *J. Catal*., **159**, 170 (1996).

Sohn, J. R., Jang, H. J. and Kim, H. W., "Catalytic Activities and Acid Strengths of NiO-ZrO_2 Catalysts Modified with Acids," *Korean J. Chem. Eng*., **7**, 7 (1990)

Sohn, J. R., Kim, H. W., Park, M. Y., Park, E. H., Kim, J. T. and Park, S. E., "Highly Active Catalyst of NiO-ZrO_2 Modified with H_2SO_4 for Ethylene Dimerization," *Appl. Catal. A: General*, **128**, 127 (1995).

Sohn, J. R., Kim, J. G., Kwon, T. D. and Park, E. H., "Characterization of Titanium Sulfate Supported on Zirconia and Activity for Acid Catalysis," *Langmuir*, **18**, 1667 (2002).

Sohn, J. R. and Ozaki, A., "Acidity of Nickel Silicate and its Bearing on the Catalytic Activity for Ethylene Dimerization and Butene Isomeriation," *J. Catal*., **61**, 29 (1980).

Sohn, J. R. and Park, M. Y., "Characterization of Zirconia-supported Tungsten Oxide Catalyst," *Langmuir*, **14**, 6140 (1998).

Sohn, J. R. and Park, W. C., "Ethylene Dimerization Catalyst of Nickel Sulfate Supported on Silica-alumina," *Korean J. Chem. Eng*., **17**, 727 (2000).

Sohn, J. R. and Park, W. C., "The Roles of Active Sites of Nickel Sulfate Supported on γ-Al_2O_3 for Ethylene Dimerization," *Appl. Catal. A: General*, **239**, 269 (2003).

Sohn, J. R., Park, W. C. and Kim, H. W., "Characterization of Nickel Sulfate Supported on γ-Al_2O_3 for Ethylene Dimerization and its Relationship to Acidic Properties," *J. Catal.*, **209**, 69 (2002).

Sohn, J. R. and Ryu, S. G., "Surface Characterization of Chromium Oxide-zirconia Catalyst," *Langmuir*, **9**, 126 (1993).

Tanabe, K., "Solid Acids and Bases," Kodansa, Tokyo (1970).

Tanabe, K., Misono, M., Ono, Y. and Hattori, J., "New Solid Acids and Bases," Elsevier Science, Amsterdam (1989).

Vaudagna, S. R., Conelli, R. A., Canavese, S. A. and Figoli, N. S., "SO_4^{2-}-ZrO_2 and Pt/SO_4^{2-}-ZrO_2: Activity and Stability During n-Hexane Isomerization," *J. Catal*., **169**, 389 (1997).

Yamaguchi, T., "Recent Progress in Solid Superacid," *Appl. Catal*., **61**, 1 (1990).